



OPEN ACCESS

EDITED BY

Nethaji Muniraj,
Children's National Hospital, United States

REVIEWED BY

Hao Sun,
Dana-Farber Cancer Institute, United States
Alessandra Trojani,
Niguarda Ca' Granda Hospital, Italy

*CORRESPONDENCE

David F. Moreno
✉ dfmoreno@clinic.cat
Carlos Fernández de Larrea
✉ cfern1@clinic.cat

†These authors have contributed
equally to this work

RECEIVED 01 April 2025
ACCEPTED 12 June 2025
PUBLISHED 01 July 2025

CITATION

Moreno DF, Nadeu F, Brasó-Maristany F,
Vaqué S, Paz S, Mañé J, Cardús O, Medina E,
Lozano E, Rodríguez-Lobato LG, de Daniel A,
Tovar N, Cibeira MT, Bladé J, Rosiñol L,
Prat A, Colomer D and Fernández de Larrea C
(2025) Genomic and immune
profiling of prognostic risk groups
in IgM gammopathy reveals novel
biomarkers beyond *MYD88* L265P.
Front. Immunol. 16:1604089.
doi: 10.3389/fimmu.2025.1604089

COPYRIGHT

© 2025 Moreno, Nadeu, Brasó-Maristany,
Vaqué, Paz, Mañé, Cardús, Medina, Lozano,
Rodríguez-Lobato, de Daniel, Tovar, Cibeira,
Bladé, Rosiñol, Prat, Colomer and Fernández
de Larrea. This is an open-access article
distributed under the terms of the [Creative
Commons Attribution License \(CC BY\)](https://creativecommons.org/licenses/by/4.0/). The
use, distribution or reproduction in other
forums is permitted, provided the original
author(s) and the copyright owner(s) are
credited and that the original publication in
this journal is cited, in accordance with
accepted academic practice. No use,
distribution or reproduction is permitted
which does not comply with these terms.

Genomic and immune profiling of prognostic risk groups in IgM gammopathy reveals novel biomarkers beyond *MYD88* L265P

David F. Moreno^{1,2*†}, Ferran Nadeu^{2,3†}, Fara Brasó-Maristany^{2,4,5},
Sergi Vaqué², Sara Paz⁶, Joan Mañé², Oriol Cardús²,
Elena Medina¹, Ester Lozano^{1,2}, Luis Gerardo Rodríguez-Lobato^{1,2},
Anna de Daniel^{1,2}, Natalia Tovar¹, María T. Cibeira¹, Joan Bladé¹,
Laura Rosiñol¹, Aleix Prat^{2,4,5,7}, Dolors Colomer^{2,3,6}
and Carlos Fernández de Larrea^{1,2*}

¹Amyloidosis and Myeloma Unit, Department of Hematology, Hospital Clínic de Barcelona, University of Barcelona, Barcelona, Spain, ²Institut d'Investigacions Biomèdiques August Pi i Sunyer (IDIBAPS), University of Barcelona, Barcelona, Spain, ³Centro de Investigación Biomédica en Red de Cáncer (CIBERONC), Madrid, Spain, ⁴Institute of Cancer and Blood Diseases, Barcelona, Spain, ⁵Reveal Genomics, Barcelona, Spain, ⁶Hematopathology Unit, Department of Pathology, Hospital Clínic de Barcelona, University of Barcelona, Barcelona, Spain, ⁷Breast Cancer Unit, Institute of Oncology (IOB)-QuirónSalud, Barcelona, Spain

Background: *MYD88* L265P is an early mutation in IgM monoclonal gammopathy of undetermined significance (MGUS) and asymptomatic Waldenström macroglobulinemia (WM). Given the high prevalence of the *MYD88* mutation observed in epidemiological studies, its presence is not sufficient to drive disease progression. In fact, a recent risk model of progression reported that the impact of other laboratory biomarkers was superior to the *MYD88* mutation's presence. Due to the low incidence of these clinicopathological entities, there is a need for a better characterization of tumor and immune cells that can help to identify novel biomarkers. We hypothesize that the characterization of the risk groups in asymptomatic patients could improve the discovery of drivers of disease progression

Methods: We characterized the genomic and immune landscape of the most recent prognostic risk categories in 19 IgM MGUS and 17 asymptomatic WM patients. We performed targeted next generation sequencing (NGS) on CD19+ cells from bone marrow samples at diagnosis using a panel of 54 lymphoma-driver genes. Whole bone marrow samples were also used to measure mRNA gene expression in tumor and immune cells using the PanCancer ImmuneProfiling panel on the nCounter platform (NanoString).

Results: We observed that low-risk patients were only characterized by the presence of *MYD88* L265P, while intermediate- and high-risk groups harbored additional mutations on *CXCR4*, *KMT2D*, *ARID1A* and *EP300*. Regarding the mRNA expression analyses, we found an increased proportion of myeloid cells in the low-risk group, with monocytes having a significant decrease in low versus high-risk patients. The high-risk group also upregulated genes involved in the

activation of NF- κ B and B-cell receptor (BCR) signaling, while low-risk patients upregulated genes associated with an alternative activation of B cells or a decrease of the BCR signaling, such as TOLLIP, CEACAM1 and CR1.

Conclusions: Beyond the *MYD88* mutation, we described novel molecular mechanisms associated with high-risk patients, as an effort moving towards easy-to-use new biomarkers in IgM gammopathy.

KEYWORDS

MGUS, Waldenström, *MYD88*, *CXCR4*, immune

Introduction

IgM monoclonal gammopathy of undetermined significance (MGUS) and Waldenström macroglobulinemia (WM) are characterized by the presence of a monoclonal IgM in serum produced by abnormal mature B cells located in the bone marrow (BM) (1, 2). The malignant B-cell clone is proportionally higher in WM compared to IgM MGUS; however, they share similar immunophenotypical and genomic characteristics. For instance, it has been described that both share the expression of CD22^{low} and CD25⁺ on abnormal B cells (3, 4), along with mutations in *MYD88* and *CXCR4* (5–8). In this sense, intensive research to categorize the risk of progression have made possible to model the progression free survival (PFS) in both IgM MGUS and WM using common biomarkers from routine clinical practice (9–12). Regarding the *MYD88* L265P impact, previous reports suggested that wild type (wt) patients, either asymptomatic or symptomatic, had worse outcomes (10, 13, 14). More recently, its independent value was put into debate in two multicenter studies, in which the mutation was not an independent predictor in asymptomatic patients (11), or did not impact in the overall survival of symptomatic patients (12). In line with these findings, the mutation burden analyzed with droplet digital polymerase chain reaction (ddPCR) showed that a high *MYD88* mutation burden was associated with higher risk of progression, rather than the presence or absence of the mutation (7).

Therefore, prognostic risk models in IgM gammopathy should include a comprehensive analysis to further improve biomarker discovery. Single cell technologies have improved the field in characterizing with great detail the cell-of-origin of the lymphoplasmacytic clones and the tumor microenvironment (TME) in IgM MGUS and WM (15–19); however, its application in the clinical setting remains challenging, as well as its prognostic validation. In the present study, we hypothesized that the addition of other somatic mutations beyond *MYD88* L265P and gene expression patterns of the clonal B cells and TME using affordable, high throughput techniques could characterize the clinical phenotypes behind the prognostic risk categories in asymptomatic patients and could serve as biomarkers of disease progression.

We characterized the clinical risk categories based on the most recent prognostic classification that relied on the presence of a serum IgM ≥ 10 g/L, BM infiltration $\geq 20\%$, β 2-microglobulin ≥ 3 mg/L and albumin < 4 g/dL. High-risk patients had at least 3 factors, while intermediate- and low-risk groups had 2, and none or 1 risk factors, respectively (11). We used a panel of genes that are recurrently altered in mature B-cell lymphomas to sequence the tumor cells of IgM gammopathy patients, followed by the characterization of the TME in response to the malignant clone, resembling the actual BM environment. We found that *CXCR4*, *ARID1A*, *KMT2D* and *EP300* mutations are present in intermediate and high-risk groups, also showing an association with the B-cell receptor (BCR) signaling. In contrast, low risk patients harbored only *MYD88* L265P and showed upregulation of genes that may interfere with BCR activation. These biomarkers can explain the differences of progression risk in IgM gammopathy patients and could be further exploited in the clinic.

Methods

Patients and sample processing

We analyzed patients with IgM MGUS and asymptomatic WM who were diagnosed between 2021 and 2022 in Hospital Clinic de Barcelona. The diagnosis was established according to the International Consensus criteria (2). All patients had bone marrow aspirates available, and only WM patients underwent a bone marrow biopsy. WM patients were not exposed to previous treatments. All patients signed an informed consent to collect BM samples in the biobank of Hospital Clinic de Barcelona, in accordance with the Declaration of Helsinki. The study was approved by the institutional review board.

The methodology followed to process the samples is described in the [Supplementary Material](#). In short, BM samples were collected in EDTA tubes for further characterization of B cells and plasma cells using multiparametric flow cytometry (MFC) ([Supplementary Table 1](#)), detection of the *MYD88* L265P by ddPCR, targeted next generation sequencing (NGS) and mRNA expression analyses.

Regarding the MFC gating strategy, CD4+, CD8+ and NK cells were quantified relative to the total CD3+ T-cell population or events. B cells and plasma cells were quantified relative to the total number of events (bone marrow cellularity). NGS was performed after CD19+ isolation by immunomagnetic beads (Milteny Biotec, Bergisch Gladbach, Germany). RNA was extracted from whole BM samples after three steps of erythrocyte lysis, centrifugation followed with the supernatant discarded to capture the signal from all immune cells.

Next generation sequencing of target genes

DNA from the CD19+ enriched samples was used for NGS using a panel of 54 target genes ([Supplementary Table 2](#)) that are recurrently mutated in mature B cell neoplasms (SOPHiA Lymphoma Solution, SOPHiA Genetics, Rolle, Switzerland). A minimum of 100 ng of DNA was used for library preparation, following the recommendations of SOPHiA Genetics. Libraries were then sequenced using 150 bp paired end reads on a NextSeq 2000 P1 instrument (Illumina, San Diego, CA, USA), with a mean coverage of 1500x. The analysis of the sequencing data is described in the [Supplementary Material](#).

Quantification of gene expression

The isolated RNA was quantified using Qubit 2.0 Fluorometer (Thermo Fisher). At least 300 ng of RNA per sample was used in the nCounter instrument (NanoString Technologies, Inc. Seattle, WA). The panel used was the PanCancer ImmuneProfiling which consisted of 730 genes that are involved in adaptive and innate immune response to cancer and 40 housekeeping genes. The analysis of the mRNA expression is described in the [Supplementary Material](#).

Statistical analyses

The chi-square test was used to compare proportions across clinical categories. The Kruskal-Wallis test was used to compare quantitative features according to diagnosis. Pearson correlation or Spearman tests were used to obtain a correlation index between numerical values. The log-rank test was used to assess the significance between conditions in PFS, and the Kaplan-Meier method to plot survival curves. For differential gene expression (DGE) analysis, a false discovery rate (q-value) of less than 0.25 was considered significant. All downstream analyses were performed using R (v. 4.4.0, R Foundation for Statistical Computing, Vienna, Austria).

Results

Clinical characteristics

A total of 36 patients (19 IgM MGUS and 17 WM) were evaluated. [Table 1](#) summarizes their clinical characteristics. WM

patients exhibited higher levels of both serum IgM and bone marrow lymphocytic infiltration, along with lower serum albumin levels compared to those with IgM MGUS. In addition, WM patients had a trend towards lower serum IgG and higher β 2-microglobulin levels than IgM MGUS. The majority of IgM MGUS and WM patients had kappa-light chain restriction, and no differences were observed regarding the plasma cell bone marrow infiltration between the two groups. All patients with WM had a clonal B-cell population detected in the BM except for one who was diagnosed with lymphoplasmacytic lymphoma in the lymph nodes. On the contrary, only 7 (36.8%) patients with IgM MGUS had a B-cell clone in the BM. The size of the B-cell clones measured by MFC was higher in WM compared to IgM MGUS (24.5% vs. 85.5%; $p < 0.001$). We also assessed the expression of antigen markers on B-cell clones that are commonly associated with IgM gammopathy. In fact, the presence of CD22^{low} (36.8% vs. 94.1%, $p < 0.001$) and CD25+ (36.8% vs. 76.5%, $p = 0.017$) were detected in both IgM MGUS and WM patients. Two patients with IgM MGUS had only clonal plasma cells without any detectable B cell clone by MFC. Regarding the MYD88 L265P detection using ddPCR or targeted NGS, the mutation was detected in 15 (78.9%) and 14 (82.4%) patients with IgM MGUS and WM, respectively. The mean MYD88 mutation burden assessed by ddPCR was 1.22% and 8.63% in patients with IgM MGUS and WM ($p < 0.001$), respectively. The MYD88 mutation burden was partially correlated with the proportion of clonal B cells ($r = 0.54$, $p < 0.001$) and plasma cells ($r = 0.40$, $p = 0.024$) in the BM detected by MFC. Seven (36.8%) MYD88 mutated IgM MGUS patients did not have any detectable clonal B or plasma cells by MFC. [Figures 1A, B](#) summarizes the processing of samples and associations between the MYD88 mutation status and MFC. According to the Spanish risk model, 78.9% and 82.4% of IgM MGUS and WM patients were categorized as intermediate or high risk, respectively. The MYD88 mutation was prevalent in 12 (80.0%) out of 15 intermediate and high-risk IgM MGUS, and 11 (78.6%) out of 14 intermediate and high-risk WM. In total, six high-risk and 3 intermediate-risk patients progressed. On the other hand, the DFCI risk model classified most patients as low and intermediate risk, with 3 high-risk, 4 intermediate-risk and 2 low-risk patients experiencing disease progression ([Figure 1C](#)). These findings led us to use the Spanish model as the framework for further analyses. After a median follow-up of 2.62 years (interquartile range [IQR] 2.32 – 3.10), high-risk patients had an increased cumulative probability of progression compared to intermediate- ($p = 0.013$) and low-risk patients ($p = 0.010$) ([Figure 1D](#)). Seven WM and 2 IgM MGUS patients experienced disease progression.

Genomic landscape of prognostic risk categories

Regarding the MYD88 status, there was no association between risk groups and the mutation prevalence (85.7%, 80.0%, 77% for low-, intermediate-, and high-risk, respectively; $p = 0.920$) assessed either by ddPCR or NGS. The mean MYD88 mutation burden by

TABLE 1 Patients' characteristics.

Patients characteristics	IgM MGUS N=19	WM N=17	P-value
Age, median (IQR)	67.6 (54.1 – 75.7)	71.7 (68.4 – 74.0)	0.4
Sex, female (%)	11 (58)	11 (65)	0.7
Serum M-protein, g/L	2.8 (0.0 – 4.1)	6.9 (4.3 – 9.9)	<0.001
Albumin, g/dL	4.5 (4.3 – 4.6)	4.2 (3.9 – 4.4)	0.012
β2-microglobulin mg/L	1.9 (1.4 – 3.2)	2.5 (2.2 – 3.2)	0.07
Serum IgM, g/L	4.0 (2.8 – 5.0)	6.7 (3.3 – 14.2)	0.03
Serum IgG, g/L	8.4 (7.4 – 10.1)	5.9 (4.8 – 9.8)	0.08
Serum IgA, g/L	1.5 (0.9 – 1.7)	1.1 (0.6 – 1.6)	0.2
Bone marrow, (%)			
Lymphocytes	11 (7 – 14)	26 (14 – 32)	0.001
Plasma cells	2 (1 – 4)	2 (1 – 4)	0.9
Kappa light chain isotype, (%)	14 (74)	13 (76)	0.9
MYD88 L265P by ddPCR, (%)	15 (78.9)	14 (82.4)	0.5
Risk category, (%)			
Low	4 (21.1)	3 (17.6)	0.10
Intermediate	13 (68.4)	7 (41.2)	
High	2 (10.5)	7 (41.2)	

The whole series was composed of 19 patients diagnosed with IgM monoclonal gammopathy of undetermined significance (MGUS) and 17 with Waldenström macroglobulinemia (WM). There were no missing values. N, number of patients; IQR, interquartile range; M-protein, serum monoclonal protein.

ddPCR was 6.0%, 1.80% and 9.9% for low-, intermediate-, and high-risk, respectively ($p=0.065$). The Pearson correlation between the MYD88 L265P VAF detected by NGS and the mutation burden by ddPCR was 0.82 ($p<0.001$) (Supplementary Figure 1A). A total of 93 mutations were detected in 34 (94.4%) patients using NGS (Supplementary Table 3). Two patients without detectable mutations by NGS were one IgM MGUS and one WM, and both were categorized as intermediate risk. The first one had a MYD88 L265P mutation burden by ddPCR of 0.12%, while the second one did not have the mutation by ddPCR. Based on diagnosis, 14 (73.7%) IgM MGUS and 14 (82.4%) WM patients had the MYD88 L265P mutation by NGS ($n=36$). The mean VAF of the MYD88 L265P by NGS was 7.81% and 29.3% in IgM MGUS and WM, respectively.

The second most frequent mutation involved was CXCR4, in which 4 (21.1%) IgM MGUS and 7 (41.1%) WM patients had at least one mutation. The mean VAF of CXCR4 mutations was 1.7% and 12.0% in IgM MGUS and WM, respectively. KMT2D mutations were prevalent in 4 (11.1%) IgM MGUS and 3 (8.3%) WM patients. Other less frequent mutations had an uneven distribution. For instance, mutations in BIRC3, BCL2, CIITA, KRAS, MEF2B, NFKBIE and NOTCH2 were only detected in IgM MGUS (Supplementary Figure 1B). The mutations in CXCR4 were detected only in intermediate- and high-risk groups, harboring also the MYD88 mutation. CXCR4 mutations encompassed frameshift and nonsense alterations such as c.1025C>A; p.Ser342* or c.1012C>T; p.Arg338*, the latter exclusively found in WM. One WM patient who was categorized as intermediate-risk presented a mutation in KMT2D and had disease progression, while 3 had IgM MGUS and were

intermediate-risk without presenting progression. ARID1A was altered in 5 (13.8%) patients, being all categorized as intermediate and high risk. Three patients who had ARID1A mutations presented disease progression. EP300 was the fifth gene most frequently altered, and the mutations were only present in intermediate and high-risk groups. EP300 c.2091T>G, previously reported in diffuse large B cell lymphoma (DLBCL) (20), was found in one IgM MGUS and one WM. No recurrent somatic mutations were found in KMT2D, ARID1A or EP300 in patients who progressed (Table 2). Regarding the number of mutations, high-risk patients had a median of 4 somatic mutations, whereas intermediate- and low-risk patients had only 3 and 2 median somatic mutations ($p=0.014$) (Figure 2).

Immune cells infiltration

We next examined the immune cell landscape. We used a previously validated gene signature to deconvolute cell types from our targeted gene expression panel, similar to other studies in solid tumors and DLBCL (21, 22). The proportion of CD8+ ($r=0.36$; $p=0.033$), NK ($r=0.42$; $p=0.010$) and CD4+ T cells ($r=0.37$; $p=0.030$) inferred from gene expression were positively correlated with that obtained from MFC (Supplementary Figures 2A–C). We excluded the inferred proportion of B cells and plasma cells to better illustrate the role of immune cells, and merged specific cell types (mast cells, macrophages, NK cells, dendritic cells and CD4 T cells) that contained multiple subtypes to increase the correlation of canonical genes from our targeted mRNA assay and the reference. We found high heterogeneity of the immune cell

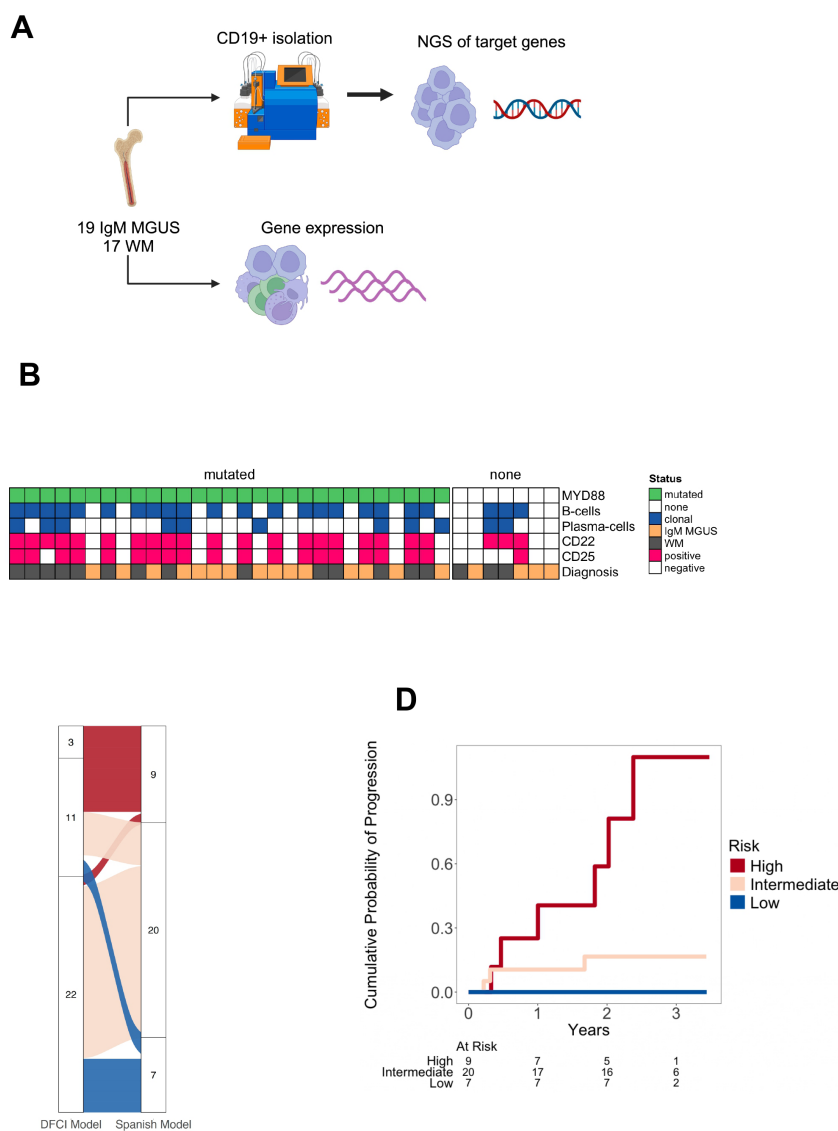


FIGURE 1 Sample processing and baseline patient's characteristics. **(A)** Whole bone marrow samples were processed with immunomagnetic sorting beads to obtain CD19+ cells followed by next generation sequencing (NGS) targeting 54 lymphoma driver genes. mRNA was obtained from whole bone marrow samples for further use in the nanoString nCounter platform using the PanCancer immunoprofiling assay. **(B)** Immunophenotypical characteristics of IgM monoclonal gammopathy of undetermined significance (MGUS) and Waldenström macroglobulinemia (WM) according to the presence of *MYD88* L265P detected by droplet digital polymerase chain reaction. **(C)** Distribution of patients based on the risk categorized by the Dana Farber Cancer Institute (DFCI) and the Spanish models. **(D)** Probability of progression based on risk categories according to the Spanish model.

infiltration in each risk group, characterized by a high proportion of myeloid cells. Meanwhile, the T-cell subpopulations represented a few percentage of the immune cell landscape in each patient. For instance, the mean infiltration rates for CD8+ T cells, monocytes, mast cells and neutrophils were 1.4%, 26.1%, 21.3% and 29.7%, respectively. Among all cell types, the monocyte infiltration showed a consecutive significant decrease from low towards high-risk patients ($p=0.040$). Of note, mast cells had an increasing trend towards high risk and represented the third most abundant immune cell type (mean of low-, intermediate-, and high-risk groups were 17.1%, 21.5% and 24.4%, respectively) (Figures 3A, B). According to

diagnosis, the proportion of monocytes, neutrophils and mast cells were similar in both IgM MGUS and WM. Although present in low counts, naïve CD4+ T cells ($p=0.022$) and dendritic cells ($p=0.037$) were increased in IgM MGUS patients. We further investigated whether the presence of the *MYD88* L265P or *CXCR4* mutations were associated with a distinct immune repertoire. The frequency of CD8+ T cells ($p=0.017$), NK cells ($p=0.048$) and mast cells ($p=0.015$) were increased in the *MYD88* mutated samples, whereas the neutrophils ($p=0.049$) proportion was decreased (Supplementary Figures 2D, E). *CXCR4* mutations was not associated with any particular cell type (data not shown).

TABLE 2 Somatic mutations (single nucleotide variants and small indels) in patients who progressed.

Patient	Diagnosis	Risk	Chromosome	Position	Reference allele	Variant allele	Gene	Coding sequence	Protein sequence	VAF (%)
PNT1	WM	High	2	136114915	G	T	<i>CXCR4</i>	c.1025C>A	p.Ser342*	10.1
PNT1	WM	High	22	41178506	TCAG	T	<i>EP300</i>	c.6798_6800delGCA	p.Gln2267del	41.2
PNT1	WM	High	3	38141150	T	C	<i>MYD88</i>	c.779T>C	p.Leu260Pro	11.1
PNT1	WM	High	X	101356177	A	G	<i>BTK</i>	c.1543T>C	p.Cys515Arg	10.3
PNT1	WM	High	X	101356177	A	T	<i>BTK</i>	c.1543T>A	p.Cys515Ser	0.9
PNT5	WM	High	3	38141150	T	C	<i>MYD88</i>	c.779T>C	p.Leu260Pro	42.5
PNT29	WM	High	4	152328358	C	A	<i>FBXW7</i>	c.1268G>T	p.Gly423Val	0.5
PNT26	WM	High	1	26774683	C	T	<i>ARID1A</i>	c.4456C>T	p.Gln1486*	65.9
PNT26	WM	High	1	116544389	TTAAGTTGTAGA	T	<i>CD58</i>	c.275_285delTCTACAACCTTA	p.Ile92fs	0.4
PNT26	WM	High	2	136114928	G	A	<i>CXCR4</i>	c.1012C>T	p.Arg338*	36.8
PNT26	WM	High	3	38141150	T	C	<i>MYD88</i>	c.779T>C	p.Leu260Pro	66.0
PNT30	WM	Intermediate	1	26731539	C	A	<i>ARID1A</i>	c.1738C>A	p.Pro580Thr	0.8
PNT30	WM	Intermediate	1	26732787	T	G	<i>ARID1A</i>	c.1915T>G	p.Leu639Val	18.5
PNT30	WM	Intermediate	12	49048002	C	T	<i>KMT2D</i>	c.4199G>A	p.Cys1400Tyr	1.1
PNT30	WM	Intermediate	17	65014258	C	T	<i>GNA13</i>	c.1133G>A	p.Ter378Ter	50.3
PNT30	WM	Intermediate	22	41146776	T	G	<i>EP300</i>	c.2091T>G	p.Ser697Arg	44.1
PNT30	WM	Intermediate	22	41170438	C	T	<i>EP300</i>	c.4319C>T	p.Pro1440Leu	18.6
PNT30	WM	Intermediate	6	137874967	TTCCGCTGGC	T	<i>TNFAIP3</i>	c.419_427delTCCGCTGGC	p.Phe140_Gln143delinsTer	21.4
PNT32	WM	High	16	3731781	T	C	<i>CREBBP</i>	c.4885A>G	p.Lys1629Glu	0.9
PNT32	WM	High	2	136114911	AGATGAATGTCCACCTCG	A	<i>CXCR4</i>	c.1012_1028delCGAGGTGGACATTCATC	p.Arg338fs	0.5
PNT32	WM	High	22	41150154	C	A	<i>EP300</i>	c.2773C>A	p.Pro925Thr	16.0
PNT32	WM	High	3	38141150	T	C	<i>MYD88</i>	c.779T>C	p.Leu260Pro	1.1
PNT32	WM	High	8	127738358	C	CCAG	<i>MYC</i>	c.154_156dupCAG	p.Gln52dup	6.4
PNT32	WM	High	9	37006497	C	T	<i>PAX5</i>	c.451G>A	p.Val151Ile	2.7
PNT35	IgM MGUS	High	1	26766292	A	G	<i>ARID1A</i>	c.2804A>G	p.Asn935Ser	1.2
PNT35	IgM MGUS	High	19	19146330	A	G	<i>MEF2B</i>	c.845T>C	p.Leu282Pro	0.2

(Continued)

TABLE 2 Continued

Patient	Diagnosis	Risk	Chromosome	Position	Reference allele	Variant allele	Gene	Coding sequence	Protein sequence	VAF (%)
PNT35	IgM MGUS	High	6	137874871	A	G	<i>TNFAIP3</i>	c.322A>G	p.Thr108Ala	1.9
PNT35	IgM MGUS	High	9	22008816	G	T	<i>CDKN2B</i>	c.138C>A	p.Phe46Leu	5.9
PNT27	IgM MGUS	Intermediate	3	38141150	T	C	<i>MYD88</i>	c.779T>C	p.Leu260Pro	0.7

MGUS, monoclonal gammopathy of undetermined significance; WM, Waldenström macroglobulinemia; VAF, variant allele frequency.

Differentially expressed genes across risk categories

In total, 110 genes were differentially expressed between high and low risk and 4 genes between high and intermediate risk (Figures 4A, B). The most significant were B-cell related genes, given the increase in the B-cell (mean 9.0%, range 0 to 42.1%) and plasma-cell (mean 2.1%, range 0 to 10%) compartments inferred from gene expression. Only the plasma cells were positively correlated between gene expression and MFC ($r=0.40$; $p=0.034$) (Supplementary Figure 2F). Genes that showed an increasing gene expression pattern from low towards high-risk groups were *BLK*, *TNFRSF13C*, *DUSP4*, *CD28*, *IL10* and *CD44*. On the contrary, *TOLLIP*, *CEACAM1* and *CR1* were upregulated in low-risk patients (Figures 4C-K). Other molecules of interest such as the *IGF1R* and *IGF2R* were downregulated in the high risk compared to the low-risk group. The expression of the immune checkpoints *CTLA4*, *TIGIT*, *LAG3*, *PD1* and *HAVCR2* did not show any differences (Supplementary Figures 3A-E). Considering the possibility of capturing gene expression signatures associated with the diagnosis rather than the risk categories, we further performed DGE analysis based on diagnosis. We did not find significant differences, except for the upregulation of *ITGA6* in IgM MGUS compared to WM (\log_2FC 0.85, $p<0.001$, q -value=0.063), that was also observed in low-risk patients in contrast to high risk (\log_2FC 1.00, $p=0.003$, q -value=0.17). No differential expressed genes were found according to *MYD88* L265P or *CXCR4*, *KMT2D* and *ARID1A* mutations.

Gene expression signatures of high and low tumor burden patients

We then performed enrichment analysis by merging low- and intermediate-risks into a single group, in contrast to high-risk. We observed that high-risk patients had a significant association with the NF- κ B signaling and an inflammatory response mediated by IFN- γ and the IL-2 mediated STAT5 activation (Figure 5A). Other signatures associated with the high-risk group were related to an inflammatory response mediated by the NF- κ B and an activation of Th1 cytotoxic cells. Meanwhile, the low-risk group was characterized by an increase of myeloid-related compartment signatures (Figure 5B), reflecting the increased proportion of monocytes and neutrophils. Using the top upregulated genes in high and low/intermediate risk groups to infer protein interactions, we found that the high-risk was associated with the BCR signaling and expression of CD22, the B cell-activating factor receptor (BAFFR or TNFRSF13C), and key components of the BCR (CD79A/B). The low and intermediate risk networks were characterized by B-cell activation based on SYK (CR1, Fc gamma receptor IIa/IIIa, LILRB2, CXCL12, IL6R) (Figures 5C, D). SYK and MAPK1 showed a continuous increase from high to low risk (Supplementary Figures 4A, B). Along with B cell markers, the intermediate and low risk groups had a strong association with CD9 and CD36 involved in macrophage phagocytosis and inflammation

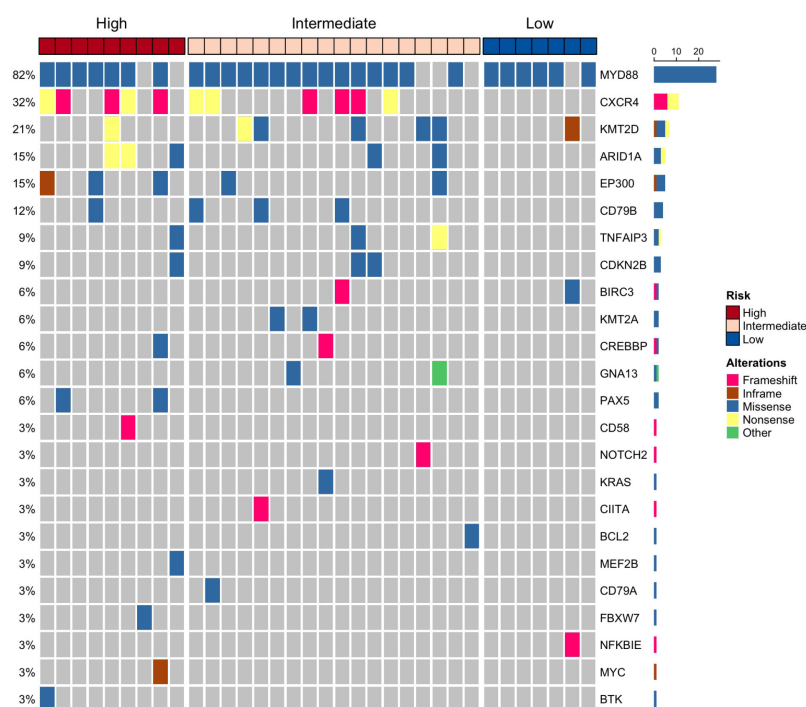


FIGURE 2

Single nucleotide variants and small indels detected by targeted next generation sequencing (NGS) in patients with IgM monoclonal gammopathy of undetermined significance (MGUS) and Waldenström macroglobulinemia (WM). In total, 34 out of 36 patients harbored mutations in driver genes by NGS.

(23, 24). To find the unique differentially expressed genes across risk groups, we obtained the significant genes ($p < 0.05$) specific for each category. High- and low-risk groups had a higher number of unique expressed genes compared to the intermediate group (Figure 6).

Discussion

We characterized the genomic and immune landscape of a recent prognostic risk classification of asymptomatic IgM gammopathy patients, as we reasoned that it could give a view of new mechanisms of progression beyond the classic biomarkers (11). We did not include previously treated WM patients due to the high heterogeneity and clonal diversification that might contribute to selection of biomarkers of treatment response instead. Given the intention of characterizing asymptomatic patients at diagnosis and the high number of IgM MGUS cases, which represented nearly half of our study population, we chose a prognostic model that included both IgM MGUS and asymptomatic WM (11), in contrast to other risk models that focused primarily on asymptomatic WM (10). Accordingly, the patients from our study were better classified in the Spanish risk model, as only intermediate and high-risk patients experienced disease progression.

Previous studies focused on the differences according to diagnosis; however, there can be challenges when comparing IgM MGUS and WM, as they share the same cell-of-origin (4, 15). In fact, we found that some IgM MGUS patients had immunophenotypical characteristics in close relationship with

WM. Clonal B cells with expression of CD22 and CD25 along with a small population of clonal plasma cells were observed in some IgM MGUS patients. Moreover, ddPCR detected the *MYD88* L265P in a high proportion of IgM MGUS patients, similar to recent reports (7, 25, 26). To note, we also observed the *MYD88* L265P mutation in IgM MGUS patients without a clonal B-cell/plasma-cell compartment in the BM, reinforcing the concept of the *MYD88* L265P as an early clonal event in IgM gammopathy (15, 16).

Beyond *MYD88* L265P, *CXCR4* mutations were exclusively identified in intermediate and high-risk groups. Among them, *CXCR4* c.1025C>A (COSV54010290) was previously reported to increase the risk of progression in asymptomatic IgM gammopathy patients (6, 7). Another reported *CXCR4* mutation in WM and other B cell neoplasms was c.1012C>T (COSV54010080) (13, 27, 28), although there is limited data on its predictive impact on progression. Frameshift mutations were also found in our intermediate and high-risk cohorts and comprised the majority of *CXCR4* mutations. A recent study suggested that *CXCR4* mutations are present only in phenotypically abnormal B cells that harbored *MYD88* L265P mutations, suggesting a potential role as driver of disease progression (15). Our results support this model, in which none of the low-risk patients harbored *CXCR4* mutations. Other mutations involving key driver genes in WM, such as *KMT2D*, *ARID1A* and *EP300*, followed a same pattern in intermediate and high-risk groups, and could be putative drivers of disease progression. For instance, a study reported that *ARID1A* mutations were associated with high BM disease burden and decreased hemoglobin values in WM patients (29, 30). In the case

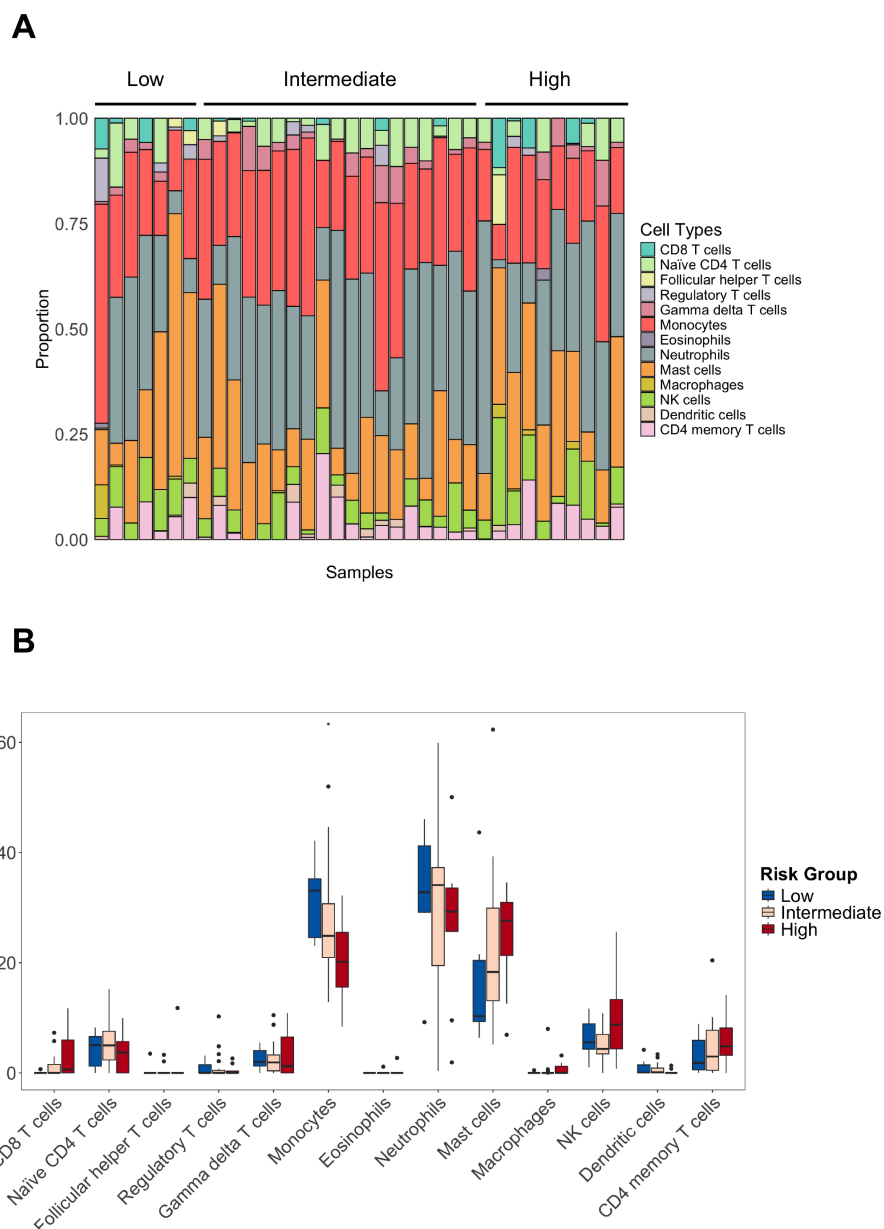


FIGURE 3 Immune cell types in IgM gammopathy. **(A)** Proportion of the cells across risk categories. B-cells and plasma cells were removed to illustrate the tumor microenvironment cells. **(B)** Distribution of cell types, showing the decrease of monocytes from low- to high-risk groups (* $p < 0.05$).

of *KMT2D*, only one study reported a prevalence of 5% in IgM MGUS and 24% in WM patients using a targeted approach (5). In our study, although *KMT2D* mutations were frequent in the intermediate risk, only one WM patient progressed with a VAF of 1.1%, and had other 6 mutations involving *ARID1A*, *EP300*, *GNA13* and *TNFAIP3*. These suggest that *KMT2D* mutations might not drive disease progression in IgM gammopathy, as they might be subclonal. We also identified mutations in *EP300* with high VAF in patients who progressed, some previously reported in DLBCL and recognized as drivers of progression (20). Moreover, another study reported an *EP300* mutation in a case of transformed WM to plasmablastic lymphoma (31). However, up to 19% of plasmablastic lymphoma patients were reported to harbor *EP300* mutations

without previous history of IgM gammopathy (32). *EP300* mutations are also prevalent in follicular lymphoma, and it has been postulated that *EP300*-mutant lymphoma cells have an abnormal germinal center transcriptional regulation (33). Altogether, our results suggest that early mutations in key epigenetic regulators such as *ARID1A*, *EP300* and *KMT2D* are present in pre-symptomatic patients with high risk of disease progression. Other recurrent mutations found in WM such as *CD79B* and *TNFAIP3* have been associated with a more aggressive phenotype and transformation to DLBCL (34, 35). While in our study patients with *CD79B* mutations had stable disease, two out of three patients who had *TNFAIP3* mutations progressed. Inactivation of *TNFAIP3* is driven by 6q deletion or

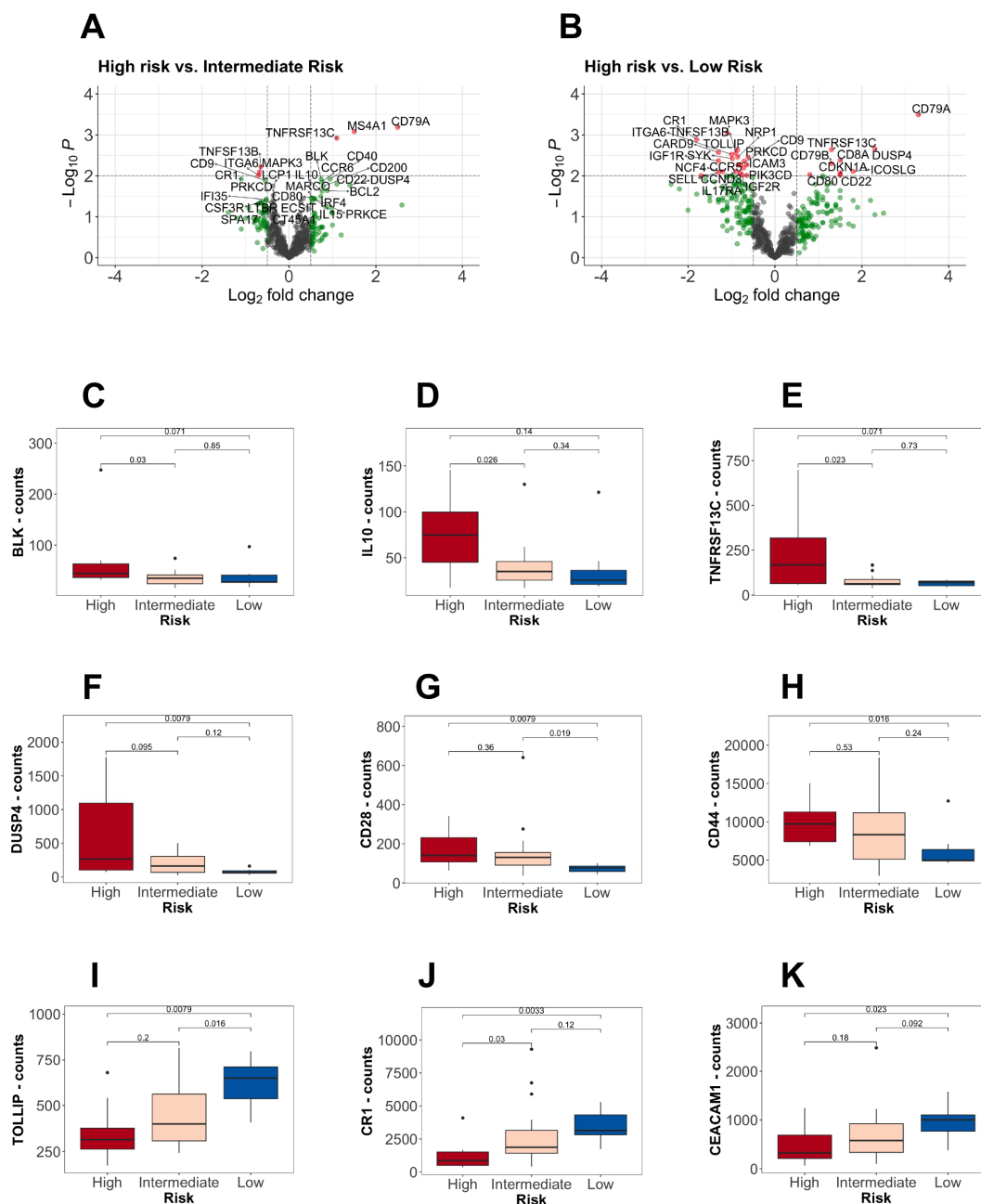


FIGURE 4
 Differential gene expression analysis according to the risk stratification. (A, B) Volcano plots showing comparisons between high-risk versus (vs.) low and intermediate-risk. On the right (positive log-fold change values), the differential expressed genes upregulated in high-risk patients. In red, the genes with a p-value lower than 0.01 and a fold change greater than 0.5. (C-H) B-cell markers upregulated in high-risk patients. (I-K) Upregulation of specific markers in low-risk patients.

mutations, and it has been associated to treatment initiation in WM (36, 37), and also reported to be present in pre-symptomatic stages such as IgM MGUS (38).

On the other hand, low allele frequency mutations (VAF 1% - 5%) involving *BIRC3*, *NOTCH2*, *BCL2*, *CIITA*, *KRAS*, *MEF2B* and *NFKBIE* were identified in IgM MGUS patients with stable disease, except for one case with *MEF2B* who progressed. Among them, *BIRC3*, *BCL2*, *MEF2B*, *NFKBIE* and *NOTCH2* were present in

MYD88 wt patients, and might have conferred a survival advantage in small clones. For instance, a study reported *NOTCH2* mutations in stable and *MYD88* wt pretreatment WM (39). Despite *BIRC3* mutations were recently identified in high risk WM patients, we were not able to associate *BIRC3* mutations to a high-risk clinical phenotype due to its only presence in IgM MGUS with low mutation burden and no disease progression (40). Another recent study did not detect mutations in *BIRC3*, *NOTCH2* and

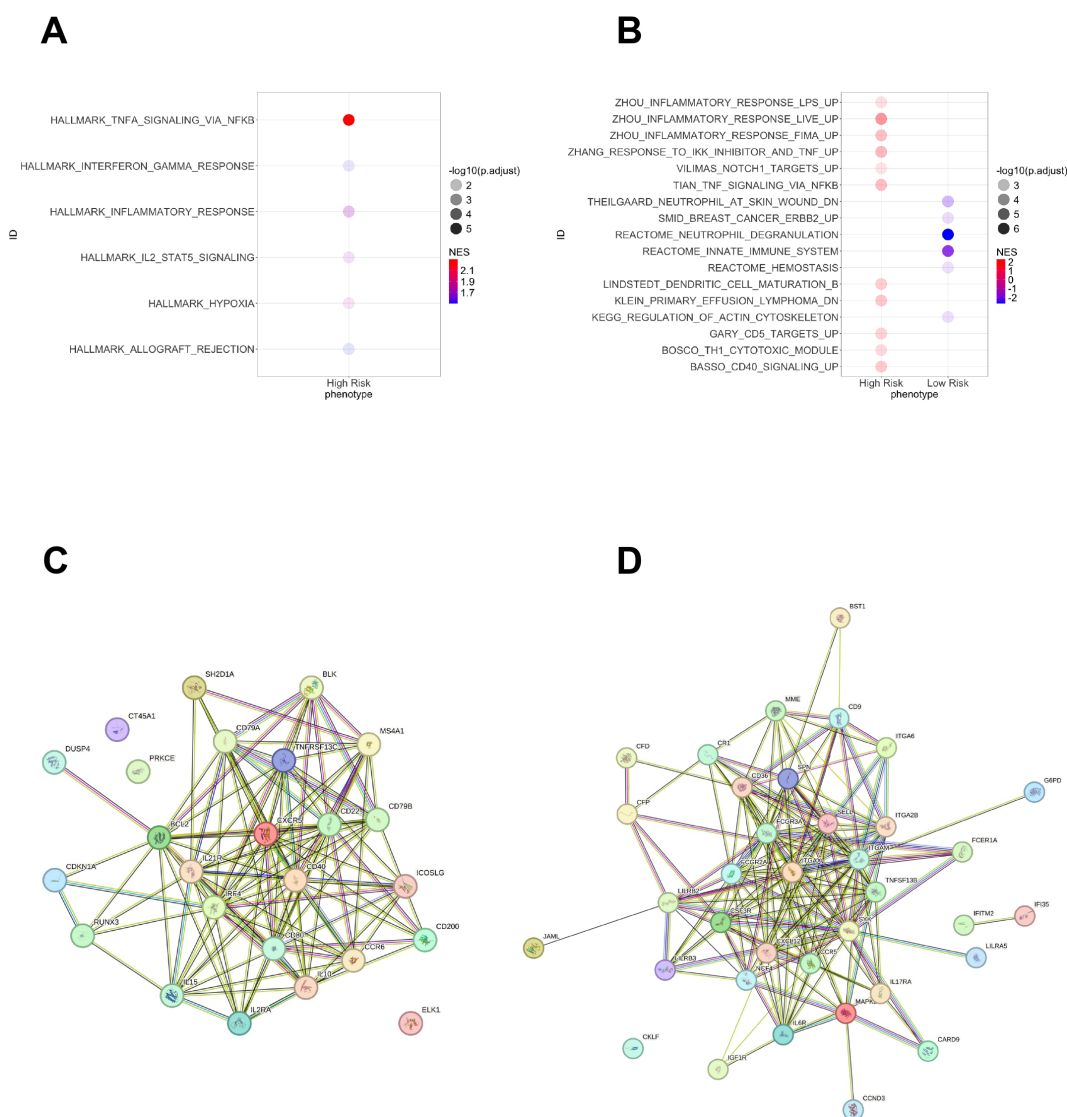


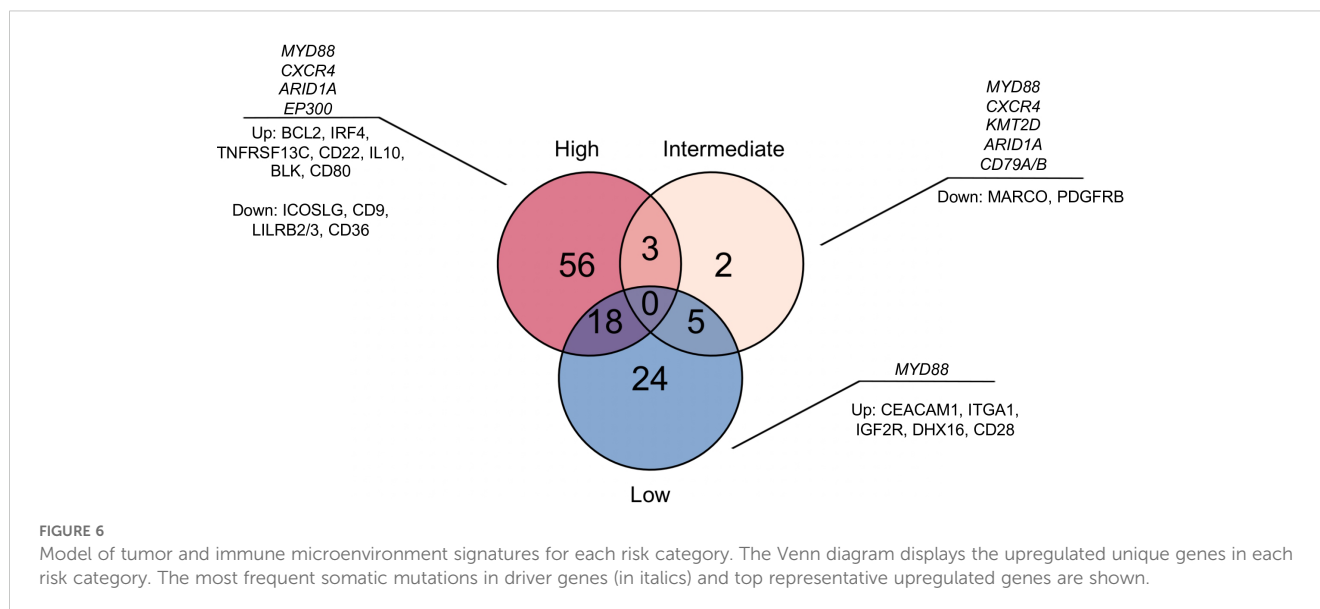
FIGURE 5 Gene set enrichment analysis in patients with high-risk IgM gammopathy and protein interaction networks. Intermediate and low risk were grouped as “low” risk patients to increase statistical power. All analyses used the Human Molecular Signatures Database. **(A)** Hallmark gene sets characteristic only in the high-risk group. **(B)** Canonical pathways gene sets comparing high and low risk. On the right of A and B are displayed the normalized enrichment score (NES). **(C)** Top upregulated genes in high-risk patients compared to intermediate and low risk. **(D)** Top upregulated genes in low-risk patients compared to high and intermediate risk.

NFKBIE in IgM MGUS or WM because their NGS assay did not cover these genomic regions (41). To what extent these mutations can further drive disease progression is yet to be investigated with larger cohorts and longer follow-up, especially in IgM MGUS patients.

Regarding the immune landscape, the low-risk group was characterized by higher proportion of myeloid cells, especially monocytes and neutrophils, and granulocytic related signatures. In line with our results, a study reported an early myeloid inflammation state in IgM MGUS and a fewer number of monocytes in WM using single cell protein screening and single cell RNA sequencing, which might contribute to a low response to interferon signaling and a compromised immune surveillance

against the tumor (16, 19). More recently, a study demonstrated the expansion of pro-tumor monocytes and how they decreased after exposure to a vaccine in a clinical trial for WM (42). Given its easy applicability and previous results in multiple myeloma and other non-Hodgkin lymphomas, further studies are needed to confirm the impact of the monocytes counts in peripheral blood on disease progression (43, 44). On the opposite, activated mast cells had an increased trend towards high-risk, findings that were previously associated with higher risk of progression in WM (45).

Genes related to the BCR signaling pathway were upregulated in high-risk patients, such as *BLK*, *CD79A*, *IRF4*, *BCL2*, *IL-10* and *CD44*. To note, we reported that *TNFRSF13C* (*BAFFR*) was upregulated in the high-risk group, an antigen that has shown



promising results as a chimeric antigen receptor (CAR) target in CD19 negative B cell malignancies (46). CD44, involved in hematopoietic cell migration, was previously associated to be overexpressed in WM and IgM MGUS compared to healthy controls, but also in *MYD88* L265P activated B-cell (ABC) DLBCL (47). In contrast, the low-risk group upregulated *CEACAM1*, *TOLLIP* and *CR1*, that are associated with a BCR signaling blockade or an alternative activation of B cells (48–50). *TOLLIP* (Toll interacting protein) is an intrinsic modulator of the Toll-like receptor that controls the NF- κ B activation mediated by *MyD88* (51). Similarly, gene set enrichment analyses identified signatures related to increased cell junctions to neighboring cells, suggesting a localized stage of the disease in low-risk patients. Although we could not find differences regarding the proportion of macrophages across the risk categories, we found overexpression of *CD9*, *CD36* and *LILRB2* in intermediate- and low-risk groups, which can translate an early metabolic alteration and altered phagocytosis, as it was previously reported the interaction of *CD9* and *CD36* on macrophage surface (23, 24).

Still, intermediate- and low-risk patients upregulated *SYK*, *MAPK1*, *IGF1R* and *IGF2R*, suggesting early proliferative B cells, which is in line with the lower amount of clonal B cells in these groups. Specific signatures related to intermediate-risk group was more difficult to assess. Although multiple mutations were also identified in the latter group, the clinical outcome for the majority of these patients were similar to the low-risk. We highlight that the intermediate group is likely a transition state, similar to a study that reported an intermediate cluster characterized by the coexistence of inflammation and tumor cell proliferation (52). Altogether, high risk patients are characterized by an increased association with the BCR signaling pathway and upregulation of *BCL2*, and low-risk patients displayed

an early immune myeloid deregulation, while trying to down regulate the activation of the NF- κ B canonical BCR signaling.

A limitation of our study was related to the follow-up time and the limited number of patients included, as it could biased the identification of a very high-risk group. On the other hand, we did not identify differences in immune checkpoints expression across risk categories, probably due to the few T-cell subpopulations in the TME in our study. However, previous studies reported only a modest expression of PD-L1 in tumor cells and PD1 in T cells in WM samples (16, 53). In addition, there is now great focus on how aberrant myeloid cells change the TME to promote tumor progression by limiting the activation of cytotoxic T cells in WM (16, 42, 54). Another limitation is that the targeted gene expression panel used in our study allowed the identification of the most representative immune cell types. Still, this approach has been previously used by others in DLBCL with high accuracy (22). Regarding the DNA sequencing, we were limited to isolate CD138+ cells due to the very low tumor burden observed in IgM MGUS. However, the high depth of the targeted design was able to identify single nucleotide variants and putative drivers of progression with high sensitivity and confidence. Further validation of our results is needed given the high heterogeneity of disease progression.

In summary, we defined the genomic and immune landscape of the risk categories in IgM gammopathy. The low-risk group is characterized by the solely presence of the *MYD88* mutation, alternative activation of B cells, early myeloid deregulation and high monocytic compartment. In contrast, the high-risk group had *CXCR4*, *ARID1A* and *EP300* somatic mutations along with a strong association with the BCR activation that might further drive disease progression.

Data availability statement

The datasets generated for this study can be found in the GSE284434 in the Gene Expression Omnibus (<https://www.ncbi.nlm.nih.gov/geo/query/acc.cgi?acc=GSE284434>). All other information is available upon reasonable request to the corresponding authors.

Ethics statement

The studies involving humans were approved by Ethics Research Committee from Hospital Clinic de Barcelona. The studies were conducted in accordance with the local legislation and institutional requirements. The participants provided their written informed consent to participate in this study.

Author contributions

DM: Conceptualization, Data curation, Formal analysis, Funding acquisition, Investigation, Methodology, Writing – original draft, Writing – review & editing. FN: Conceptualization, Data curation, Formal analysis, Validation, Writing – original draft, Writing – review & editing. FB-M: Conceptualization, Formal analysis, Writing – original draft, Writing – review & editing. SV: Writing – original draft, Writing – review & editing. SP: Writing – original draft, Writing – review & editing. JM: Conceptualization, Writing – original draft, Writing – review & editing. OC: Conceptualization, Writing – original draft, Writing – review & editing. EM: Conceptualization, Writing – original draft, Writing – review & editing. EL: Conceptualization, Writing – original draft, Writing – review & editing. LR-L: Writing – original draft, Writing – review & editing. AD: Writing – original draft, Writing – review & editing. NT: Writing – original draft, Writing – review & editing. MC: Writing – original draft, Writing – review & editing. JB: Writing – original draft, Writing – review & editing. LR: Writing – original draft, Writing – review & editing. AP: Resources, Writing – original draft, Writing – review & editing. DC: Formal analysis, Resources, Writing – original draft, Writing – review & editing. CF: Conceptualization, Funding acquisition, Investigation, Methodology, Resources, Validation, Writing – original draft, Writing – review & editing.

Funding

The author(s) declare that financial support was received for the research and/or publication of this article. This study was supported by research funding from the Spanish Institute of Health Carlos III (PI22/00647), the Asociación Española Contra el Cáncer (LABAE21971FERN), AGAUR (Generalitat de Catalunya) (2021SGR01292). DM acknowledges research support by an unrestricted grant from Janssen, the II Predoctoral Precision Oncology Grant by IOP, the Seed Money Grant and the Kyle Award

by the International Waldenström Macroglobulinemia Foundation. FN acknowledges research support from the European Hematology Association (EHA Junior Research Grant 2021, RG-202012-00245) and Sociedad Española de Hematología y Hemoterapia (SEHH).

Conflict of interest

DM received travel grants and honoraria from Janssen. FN received honoraria from Janssen, AbbVie, AstraZeneca, and SOPHiA GENETICS, and research funding from Gilead. FN licensed the use of the protected IgCaller algorithm for SOPHiA GENETICS and Diagnóstica Longwood. CF consulted and received honoraria from GSK, Sanofi, Pfizer, BeiGene, Amgen, BMS, and Janssen and received research funding from GSK, Amgen, and Janssen. JB received honoraria for lectures from Janssen and Sanofi. NT received honoraria for lectures from Pfizer. FB-M. refers a part-time employment from Reveal Genomics. AP reports advisory and consulting fees from AstraZeneca, Roche, Pfizer, Novartis, Daiichi Sankyo, Ona Therapeutics, and Peptomyc, lecture fees from AstraZeneca, Roche, Novartis, and Daiichi Sankyo, institutional financial interests from AstraZeneca, Novartis, Roche, and Daiichi Sankyo; and is a stockholder and employee of Reveal Genomics. LR received honoraria for lectures from Janssen, BMS, Amgen, Takeda, Sanofi, GSK, Pfizer and Menarini. LR-L. received honoraria and travel grants from Janssen, Amgen, BMS, GSK, Menarini Stemline, and Sanofi. MC received honoraria from Amgen and Janssen. AD received honoraria for lectures from Janssen, travel grants from Sanofi and Binding Site.

The remaining authors declare that the research was conducted in the absence of any commercial or financial relationships that could be construed as a potential conflict of interest.

The author(s) declared that they were an editorial board member of *Frontiers*, at the time of submission. This had no impact on the peer review process and the final decision.

Generative AI statement

The author(s) declare that no Generative AI was used in the creation of this manuscript.

Publisher's note

All claims expressed in this article are solely those of the authors and do not necessarily represent those of their affiliated organizations, or those of the publisher, the editors and the reviewers. Any product that may be evaluated in this article, or claim that may be made by its manufacturer, is not guaranteed or endorsed by the publisher.

Supplementary material

The Supplementary Material for this article can be found online at: <https://www.frontiersin.org/articles/10.3389/fimmu.2025.1604089/full#supplementary-material>

References

- Owen RG, Treon SP, Al-Katib A, Fonseca R, Greipp PR, McMaster ML, et al. Clinicopathological definition of Waldenström's macroglobulinemia: Consensus Panel Recommendations from the Second International Workshop on Waldenström's Macroglobulinemia. *Semin Oncol.* (2003) 30:110–5. doi: 10.1053/sonc.2003.50082
- Campo E, Jaffe ES, Cook JR, Quintanilla-Martinez L, Swerdlow SH, Anderson KC, et al. The international consensus classification of mature lymphoid neoplasms: a report from the clinical advisory committee. *Blood.* (2022) 140:1229–53. doi: 10.1182/blood.2022015851
- Paiva B, Montes MC, García-Sanz R, Ocio EM, Alonso J, De Las Heras N, et al. Multiparameter flow cytometry for the identification of the Waldenström's clone in IgM-MGUS and Waldenström's Macroglobulinemia: new criteria for differential diagnosis and risk stratification. *Leukemia.* (2014) 28:166–73. doi: 10.1038/leu.2013.124
- Paiva B, Corchete LA, Vidriales M-B, García-Sanz R, Perez JJ, Aires-Mejia I, et al. The cellular origin and Malignant transformation of Waldenström macroglobulinemia. *Blood.* (2015) 125:2370–80. doi: 10.1182/blood-2014-09-602565
- Varettoni M, Zibellini S, DeFrancesco I, Ferretti VV, Rizzo E, Malcovati L, et al. Pattern of somatic mutations in patients with Waldenström macroglobulinemia or IgM monoclonal gammopathy of undetermined significance. *Haematologica.* (2017) 102:7077–85. doi: 10.3324/haematol.2017.172718
- Xu L, Hunter ZR, Tsakmakis N, Cao Y, Yang G, Chen J, et al. Clonal architecture of CXCR4 WHIM-like mutations in Waldenström Macroglobulinaemia. *Br J Haematol.* (2016) 172:735–44. doi: 10.1111/bjh.13897
- Moreno DF, López-Guerra M, Paz S, Oliver-Caldés A, Mena M, Correa JG, et al. Prognostic impact of MYD88 and CXCR4 mutations assessed by droplet digital polymerase chain reaction in IgM monoclonal gammopathy of undetermined significance and smoldering Waldenström macroglobulinaemia. *Br J Haematol.* (2023) 200:187–96. doi: 10.1111/bjh.18502
- Treon SP, Tedeschi A, San-Miguel J, García-Sanz R, Anderson KC, Kimby E, et al. Report of consensus Panel 4 from the 11th International Workshop on Waldenström's macroglobulinemia on diagnostic and response criteria. *Semin Hematol.* (2023) 60:97–106. doi: 10.1053/j.seminhematol.2023.03.009
- Moreno DF, Pereira A, Tovar N, Cibeira MT, Magnano L, Rozman M, et al. Defining an ultra-low risk group in asymptomatic IgM monoclonal gammopathy. *Cancers.* (2021) 13:2055. doi: 10.3390/cancers13092055
- Bustoros M, Sklavinitis-Pistofidis R, Kapoor P, Liu C-J, Kastritis E, Zanwar S, et al. Progression risk stratification of asymptomatic Waldenström macroglobulinemia. *J Clin Oncol.* (2019) 37:1403–11. doi: 10.1200/JCO.19.00394
- Moreno DF, Jiménez C, Escalante F, Askari E, Castellanos-Alonso M, Arnao M, et al. Prognostic risk and survival of asymptomatic IgM monoclonal gammopathy: Results from a Spanish Multicenter Registry. *HemaSphere.* (2024) 8:e70029. doi: 10.1002/hem3.70029
- Zanwar S, Le-Rademacher J, Durot E, D'Sa S, Abeykoon JP, Mondello P, et al. Simplified risk stratification model for patients with Waldenström macroglobulinemia. *J Clin Oncol.* (2024) 42:2527–36. doi: 10.1200/JCO.23.02066
- Treon SP, Cao Y, Xu L, Yang G, Liu X, Hunter ZR. Somatic mutations in MYD88 and CXCR4 are determinants of clinical presentation and overall survival in Waldenström macroglobulinemia. *Blood.* (2014) 123:2791–6. doi: 10.1182/blood-2014-01-550905
- Treon SP, Gustine J, Xu L, Manning RJ, Tsakmakis N, Demos M, et al. MYD88 wild-type Waldenström Macroglobulinaemia: differential diagnosis, risk of histological transformation, and overall survival. *Br J Haematol.* (2018) 180:374–80. doi: 10.1111/bjh.15049
- Rodríguez S, Celay J, Goicoechea I, Jimenez C, Botta C, Garcia-Barchino M-J, et al. Preneoplastic somatic mutations including MYD88^{L265P} in lymphoplasmacytic lymphoma. *Sci Adv.* (2022) 8:eabl4644. doi: 10.1126/sciadv.abl4644
- Kaushal A, Nooka AK, Carr AR, Pendleton KE, Barwick BG, Manalo J, et al. Aberrant extrafollicular B cells, immune dysfunction, myeloid inflammation, and myD88-mutant progenitors precede Waldenström macroglobulinemia. *Blood Cancer Discov.* (2021) 2:600–15. doi: 10.1158/2643-3230.BCD-21-0043
- Bagratuni T, Aktipi F, Theologi O, Sakkou M, Verrou KM, Mavrianou-Koutsoukou N, et al. Single-cell analysis of MYD88^{L265P} and MYD88^{WT} Waldenström macroglobulinemia patients. *HemaSphere.* (2024) 8:e27. doi: 10.1002/hem3.27
- Sun H, Fang T, Wang T, Yu Z, Gong L, Wei X, et al. Single-cell profiles reveal tumor cell heterogeneity and immunosuppressive microenvironment in Waldenström macroglobulinemia. *J Transl Med.* (2022) 20:576. doi: 10.1186/s12967-022-03798-6
- Sklavinitis-Pistofidis R, Konishi Y, Heilpern-Mallory D, Wu T, Tsakmakis N, Aranha MP, et al. Single-cell RNA sequencing defines distinct disease subtypes and reveals hypo-responsiveness to interferon in asymptomatic Waldenström's Macroglobulinemia. *Nat Commun.* (2025) 16:1480. doi: 10.1038/s41467-025-56323-w
- De Groen RA, Van Eijk R, Boehringer S, Van Wezel T, Raghoo R, Ruano D, et al. Frequent mutated B2M, EZH2, IRF8, and TNFRSF14 in primary bone diffuse large B-cell lymphoma reflect a GCB phenotype. *Blood Adv.* (2021) 5(19):3760–75. doi: 10.1182/bloodadvances.2021005215
- Yao Y, Yan Z, Lian S, Wei L, Zhou C, Feng D, et al. Prognostic value of novel immune-related genomic biomarkers identified in head and neck squamous cell carcinoma. *J Immunother Cancer.* (2020) 8:e000444. doi: 10.1136/jitc-2019-000444
- Autio M, Leivonen SK, Brück O, Mustjoki S, Mészáros Jørgensen J, Marja-Liisa Karjalainen-Lindsberg ML, et al. Immune cell constitution in the tumor microenvironment predicts the outcome in diffuse large B-cell lymphoma. *Haematologica.* (2020) 106:718–29. doi: 10.3324/haematol.2019.243626
- Huang W, Febbraio M, Silverstein RL. CD9 tetraspanin interacts with CD36 on the surface of macrophages: A possible regulatory influence on uptake of oxidized low density lipoprotein. *PLoS One.* (2011) 6:e29092. doi: 10.1371/journal.pone.0029092
- Huang W, Li R, Zhang J, Cheng Y, Ramakrishnan DP, Silverstein RL. A CD36 transmembrane domain peptide interrupts CD36 interactions with membrane partners on macrophages and inhibits atherogenic functions. *Transl Res.* (2023) 254:68–76. doi: 10.1016/j.trsl.2022.10.005
- Drandi D, Genuardi E, Dogliotti I, Ferrante M, Jiménez C, Guerrini F, et al. Highly sensitive MYD88^{L265P} mutation detection by droplet digital polymerase chain reaction in Waldenström macroglobulinemia. *Haematologica.* (2018) 103:1029–37. doi: 10.3324/haematol.2017.186528
- Ferrante M, Furlan D, Zibellini S, Borriero M, Candido C, Sahnane N, et al. MYD88L265P detection in IgM monoclonal gammopathies: methodological considerations for routine implementation. *Diagnostics.* (2021) 11:779. doi: 10.3390/diagnostics11050779
- Poulain S, Roumier C, Venet-Caillaud A, Figeac M, Herbaux C, Marot G, et al. Genomic landscape of CXCR4 mutations in Waldenström macroglobulinemia. *Clin Cancer Res.* (2016) 22:1480–8. doi: 10.1158/1078-0432.CCR-15-0646
- Lacy SE, Barrans SL, Beer PA, Painter D, Smith AG, Roman E, et al. Targeted sequencing in DLBCL, molecular subtypes, and outcomes: a Haematological Malignancy Research Network report. *Blood.* (2020) 135:1759–71. doi: 10.1182/blood.2019003535
- Hunter ZR, Xu L, Yang G, Zhou Y, Liu X, Cao Y, et al. The genomic landscape of Waldenström macroglobulinemia is characterized by highly recurring MYD88 and WHIM-like CXCR4 mutations, and small somatic deletions associated with B-cell lymphomagenesis. *Blood.* (2014) 123:1637–46. doi: 10.1182/blood-2013-09-525808
- Hunter ZR, Xu L, Yang G, Tsakmakis N, Vos JM, Liu X, et al. Transcriptome sequencing reveals a profile that corresponds to genomic variants in Waldenström macroglobulinemia. *Blood.* (2016) 128:827–38. doi: 10.1182/blood-2016-03-708263
- Castillo JJ, LaMacchia J, Flynn CA, Sarosiek S, Pozdnyakova O, Treon SP. Plasmablastic lymphoma transformation in a patient with Waldenström macroglobulinemia treated with ibrutinib. *Br J Haematol.* (2021) 195:466–8. doi: 10.1111/bjh.17759
- Ramis-Zaldivar JE, Gonzalez-Farre B, Nicolae A, Pack S, Clot G, Nadeu F, et al. MAPK and JAK-STAT pathways dysregulation in plasmablastic lymphoma. *Haematologica.* (2021) 106:2682–93. doi: 10.3324/haematol.2020.271957
- Meyer SN, Scuoppo C, Vlassevka S, Bal E, Holmes AB, Holloman M, et al. Unique and shared epigenetic programs of the CREBBP and EP300 acetyltransferases in germinal center B cells reveal targetable dependencies in lymphoma. *Immunity.* (2019) 51:535–547.e9. doi: 10.1016/j.immuni.2019.08.006
- Wenzl K, Manske MK, Sarangi V, Asmann YW, Greipp PT, Schoon HR, et al. Loss of TNFAIP3 enhances MYD88L265P-driven signaling in non-Hodgkin lymphoma. *Blood Cancer J.* (2018) 8:97. doi: 10.1038/s41408-018-0130-3
- Berendsen MR, Van Bladel DAG, Hesius E, Berganza Iruquieta C, Rijntjes J, Van Spruiel AB, et al. Clonal relationship and mutation analysis in lymphoplasmacytic lymphoma/Waldenström macroglobulinemia associated with diffuse large B-cell lymphoma. *HemaSphere.* (2023) 7:e976. doi: 10.1097/HS9.0000000000000976
- Forgeard N, Baron M, Caron J, Boccon-Gibod C, Krzisch D, Guedes N, et al. Inflammation in Waldenström macroglobulinemia is associated with 6q deletion and need for treatment initiation. *Haematologica.* (2022) 107:2720–4. doi: 10.3324/haematol.2022.281053
- García-Sanz R, García-Álvarez M, Medina A, Askari E, González-Calle V, Casanova M, et al. Clonal architecture and evolutionary history of Waldenström's macroglobulinemia at the single-cell level. *Dis Model Mech.* (2023) 16:dmm050227. doi: 10.1242/dmm.050227
- García-Sanz R, Dogliotti I, Zaccaria GM, Ocio EM, Rubio A, Murillo I, et al. 6q deletion in Waldenström macroglobulinaemia negatively affects time to transformation and survival. *Br J Haematol.* (2021) 192:843–52. doi: 10.1111/bjh.17028
- Maclachlan KH, Bagratuni T, Kastritis E, Ziccheddu B, Lu S, Yellapantula V, et al. Waldenström macroglobulinemia whole genome reveals prolonged germinal center activity and late copy number aberrations. *Blood Adv.* (2023) 7:971–81. doi: 10.1182/bloodadvances.2022008876
- Østergaard S, Schejbel L, Breinholt MF, Pedersen MØ, Hammer T, Munksgaard L, et al. Mutational landscape in Waldenström macroglobulinemia evaluated using a next-

- generation sequencing lymphoma panel in routine clinical practice. *Leuk Lymphoma*. (2024) 65:758–67. doi: 10.1080/10428194.2024.2313623
41. Trojani A, Beghini A, Bossi LE, Stefanucci MR, Palumbo C, Greco A, et al. Mutational landscape of bone marrow CD19 and CD138 cells in waldenström macroglobulinemia (WM) and IgM monoclonal gammopathy of undetermined significance (IgM MGUS). *Cancer Med*. (2024) 13:e70525. doi: 10.1002/cam4.70525
42. Szymura SJ, Wang L, Zhang T, Cha S, Song J, Dong Z, et al. Personalized neoantigen vaccines as early intervention in untreated patients with lymphoplasmacytic lymphoma: a non-randomized phase 1 trial. *Nat Commun*. (2024) 15:6874. doi: 10.1038/s41467-024-50880-2
43. Tadmor T, Bari A, Sacchi S, Marcheselli L, Liardo EV, Avivi I, et al. Monocyte count at diagnosis is a prognostic parameter in diffuse large B-cell lymphoma: results from a large multicenter study involving 1191 patients in the pre- and post-rituximab era. *Haematologica*. (2014) 99:125–30. doi: 10.3324/haematol.2013.088161
44. Edwards CV, Hassan H, Yildirim C, Ferri G, Verma KP, Murray Horwitz ME, et al. Peripheral blood monocyte count is a dynamic prognostic biomarker in multiple myeloma. *Blood Adv*. (2023) 7:482–90. doi: 10.1182/bloodadvances.2022008021
45. Lemal R, Poulain S, Ledoux-Pilon A, Veronese L, Tchirkov A, Lebecque B, et al. Mast cell density and its clinical relevance in Waldenström's macroglobulinemia. *EJHaem*. (2022) 3:371–8. doi: 10.1002/jha.2378
46. Wong DP, Roy NK, Zhang K, Anukanth A, Asthana A, Shirkey-Son NJ, et al. A BAFF ligand-based CAR-T cell targeting three receptors and multiple B cell cancers. *Nat Commun*. (2022) 13:217. doi: 10.1038/s41467-021-27853-w
47. Turi M, Anilkumar Sithara A, Hofmanová L, Žihala D, Radhakrishnan D, Vdovin A, et al. Transcriptome analysis of diffuse large B-cell lymphoma cells inducibly expressing myD88 L265P mutation identifies upregulated CD44, LGALS3, NFKBIZ, and BATF as downstream targets of oncogenic NF-κB signaling. *Int J Mol Sci*. (2023) 24:5623. doi: 10.3390/ijms24065623
48. Tsugawa N, Yamada D, Watabe T, Onizawa M, Wang S, Nemoto Y, et al. CEACAM1 specifically suppresses B cell receptor signaling-mediated activation. *Biochem Biophys Res Commun*. (2021) 535:99–105. doi: 10.1016/j.bbrc.2020.11.126
49. Khairnar V, Duhan V, Maney SK, Honke N, Shaabani N, Pandya AA, et al. CEACAM1 induces B-cell survival and is essential for protective antiviral antibody production. *Nat Commun*. (2015) 6:6217. doi: 10.1038/ncomms7217
50. Malecka A, Østlie I, Trøen G, Malecki J, Delabie J, Tierens A, et al. Gene expression analysis revealed downregulation of complement receptor 1 in clonal B cells in cold agglutinin disease. *Clin Exp Immunol*. (2024) 216:45–54. doi: 10.1093/cei/uxad135
51. Capelluto DGS. Tollip: a multitasking protein in innate immunity and protein trafficking. *Microbes Infect*. (2012) 14:140–7. doi: 10.1016/j.micinf.2011.08.018
52. Mondello P, Paludo J, Novak JP, Wenzl K, Yang Z-Z, Jalali S, et al. Molecular clusters and tumor-immune drivers of IgM monoclonal gammopathies. *Clin Cancer Res*. (2023) 29:957–70. doi: 10.1158/1078-0432.CCR-22-2215
53. Jalali S, Price-Troska T, Paludo J, Villasboas J, Kim H-J, Yang Z-Z, et al. Soluble PD-1 ligands regulate T-cell function in Waldenström macroglobulinemia. *Blood Adv*. (2018) 2:1985–97. doi: 10.1182/bloodadvances.2018021113
54. Bhardwaj V, Yang Z-Z, Mukherjee P, Mudappathi R, Wang J, Tang X, et al. Polymorphonuclear myeloid-derived suppressor cells promote tumor cell survival and suppress cytotoxic T- cells in waldenström macroglobulinemia. *Blood*. (2024) 144:5661–1. doi: 10.1182/blood-2024-208966